coatings

MDPI

Article

Aluminum-Modified Plasma Nitriding with High Efficiency and Enhanced Performance

Ze He [1], Wei Wei [1,2], Jing Hu [1,2,*] and Jingyi Gu [1,3,*]

[1] Jiangsu Key Laboratory of Materials Surface Science and Technology, Changzhou University, Changzhou 213164, China; heze1@cczu.edu.cn (Z.H.); weiwei@cczu.edu.cn (W.W.)
[2] Huaide College, Changzhou University, Jingjiang 214500, China
[3] Restoration Department, Changzhou Stomatological Hospital, Changzhou 213003, China
* Correspondence: jinghoo@126.com (J.H.); gujingyi@126.com (J.G.); Tel.: +86-0519-86330095 (J.H.); +86-0519-86804028 (J.G.)

Abstract: Aluminum-modified plasma nitriding was developed in this research by the addition of a few FeAl particles around samples of 42CrMo middle carbon alloy steel during plasma nitriding. The goal of this study was to enhance nitriding efficiency and the combined performance of the steel. The research results show that nitriding efficiency was greatly enhanced, by about 6 times, with the effective hardening layer rising from 224 μm to 1246 μm compared with traditional plasma nitriding at 520 °C/4 h. More importantly, the compound layer increased just a little bit, from 11.64 μm to 14.32 μm, which remarkably reduced the ratio of the compound layer's thickness to the effective hardening layer's thickness, thus being quite beneficial to decreasing the brittleness level, making the brittleness level decrease from Level 4 to Level 1. Also, extremely high surface hardness and excellent wear resistance were obtained by aluminum-modified plasma nitriding due to the formation of hard phases of AlN and FeAl in the nitrided layer, with the surface hardness rising from 755 $HV_{0.025}$ to 1251 $HV_{0.025}$ and the wear rate reducing from 8.15×10^{-5} $g \cdot N^{-1} \cdot m^{-1}$ to 4.07×10^{-5} $g \cdot N^{-1} \cdot m^{-1}$. In other words, compared with traditional plasma nitriding, wear resistance was enhanced by two times after aluminum-modified plasma nitriding. Therefore, this study can provide comprehensive insights into the surface characteristics and combined performance of aluminum-modified plasma nitriding layers.

Keywords: plasma nitriding; effective hardening layer; compound layer; wear behavior; nitriding efficiency

Citation: He, Z.; Wei, W.; Hu, J.; Gu, J. Aluminum-Modified Plasma Nitriding with High Efficiency and Enhanced Performance. *Coatings* **2024**, *14*, 1373. https://doi.org/10.3390/coatings14111373

Academic Editor: Angela De Bonis

Received: 20 September 2024
Revised: 10 October 2024
Accepted: 23 October 2024
Published: 29 October 2024

1. Introduction

Since the majority of failures such as fatigue fracture, wear, and corrosion originate from the surface of metal components, it is of great value to apply some surface modification to enhance the properties of surfaces and bring about extreme service performance for metal components. Through surface modification, the ultimate performance of metal components can be obtained so as to save advanced raw material resources, reduce manufacturing costs, and promote the development needs of the "two-carbon" strategy [1–3].

Plasma nitriding is a typical environmentally friendly surface modification technology which has been widely used in metal components to improve their surface properties [4–6]. However, plain carbon steel and low alloy steels are not quite suitable for traditional plasma nitriding in some applications, since an excessively thick compound layer can be formed once the effective hardening layer meets the requirements, which can easily result in premature failure due to the thicker compound layer cracking [7–10].

Generally, a nitrided layer is composed of a compound layer (also called bright layer) on the top surface and a diffusion layer beneath. Since the compound layer has a different crystal structure from the diffusion layer, the two layers are difficult to deform coordinately. Thus, a thick compound layer is very likely to crack while being subjected to heavy impact

loads, resulting in premature crack failure [11–13], and a thick effective hardening layer is necessary to enhance resistance to heavy impact loads.

Because of the above reasons, it is necessary to obtain a plasma nitriding layer with a thicker effective hardening layer and thinner compound layer to meet the service requirements in practical applications, especially for components subjected to heavy impact loads. The following two ways are the traditional methods for making a compound layer become thinner: one is adjusting the nitriding parameters, including nitriding temperature, duration, or nitrogen potential to obtain a thinner nitrided layer [14–16], and the other is grinding the very surface layer to reduce the compound layer thickness [17,18]. Unfortunately, the first way is generally accompanied by a thin effective hardening layer, which brings about lower surface hardness and poorer wear performance, thus making it hard to meet the requirements of long service life for components subjected to heavy impact loads, although the premature cracks can be avoided [19,20]. And the second way is extremely hard to control and conduct due to the very high hardness and brittleness of the compound layer.

By comparing the characteristics of a nitriding layer obtained under the same condition for different kinds of steels with different amounts of alloy elements and similar carbon content, e.g., 45 steel, 42CrMo, and H13, it was found that the compound layer became thinner and the effective hardening layer became thicker with an increase in the content of alloying elements [21–23]. Thus, a prediction can be made that adding alloy elements during plasma nitriding may have an effect on the thinning of the compound layer and the thickening of the effective hardening layer.

Since aluminum is the strongest nitride-forming element, and it is used as an alloying element in typical nitrided steel of 38CrMoAl to enhance the nitriding performance [24,25]. It was found in our previous research that a higher nitriding efficiency and better performance can be obtained by depositing an aluminum hydroxide film on the surface of samples by electrolyzing aluminum nitrate [26]. Unfortunately, the adopted method of introducing an aluminum source prior to plasma nitriding is not environmentally friendly and is complicated. Thus, in this study, a simple and environmentally friendly aluminum-modified plasma nitriding technology was developed by the addition of a few FeAl particles during the plasma nitriding process, and the effect of aluminum modification on the nitriding efficiency and performance of 42CrMo alloy steel was investigated and compared with those achieved by conventional plasma nitriding.

2. Materials and Methods

Quenched and tempered 42CrMo middle carbon alloy steel with a hardness of about 320 HV was used in this research and its chemical composition is shown in Table 1. Samples were machined to dimensions of 10 mm × 10 mm× 5 mm, ground step by step using different grades of sandpaper, and then subjected to ultrasonic cleaning in alcohol for 10 min.

Table 1. Chemical composition of 42CrMo steel wt./%.

C	Cr	Mo	Mn	Si	S	P	Fe
0.42	0.92	0.20	0.85	0.30	0.011	0.014	Balance

Plasma nitriding was carried out at a temperature of 520 °C for 0.5–4 h in a mixture gas of N_2 +H_2, with the ratio of N_2:H_2 being 1:3 and with a gas pressure of 400 Pa, followed by furnace cooling. A few FeAl particles with a diameter of about 1 mm were put around the samples for aluminum-modified plasma nitriding, and the number of FeAl particles was 10 mg per square min-meters of the samples' surface area, i.e., 10 mg/mm^2. Meanwhile, traditional plasma nitriding with the same conditions, including temperature, process duration time, mixture gas, and pressure, was also conducted as a reference for a comparative study. In order to investigate the weight change after different kind of nitriding, the weight of the samples before and after plasma nitriding was weighed using

an MST-5000 electronic balance (sourced from Nidao Mechanical and Electrical Engineering Co., LTD, Shanghai, China), and the weight change was calculated for both cases.

The cross-sectional microstructure was observed by a DMI-3000M optical microscope (sourced from LEICA Company, Germany), and the compound layer thickness was obtained by measuring the bright white layer on the cross-sectional microstructure. Each layer's thickness value was determined by averaging at least five measurements to ensure reliability. The phase compositions were detected by D/max-2500 X-ray diffractometer (sourced from Rigaku Corporation, Japan) with Cu-Kα radiation (λ = 1.54 Å) under a scanning speed of 1°/min with a 0.02°step size. The surface morphology and micro-regional chemical composition were characterized by a scanning electron microscope (SEM, ZEISS EVO 18, Jena, Germany) equipped with energy dispersive spectroscopy (EDS). Meanwhile, the 3D surface topography and roughness of the nitrided specimens was characterized by DMA8000 Laser confocal microscope (sourced from LEICA Company, Wetzlar, Germany) at a magnification of 100×.

The cross-sectional microhardness was measured by HXD-1000TMC Vickers hardness tester (sourced from Optical Equipments Co., LTD, Shanghai, China) with a load of 50 g and a holding duration of 15 s. Each hardness value was determined by averaging at least three measurements to ensure reliable value. Meanwhile, according to the Chinese national standard [27], the brittleness level of the nitriding layer was evaluated based on the cracking extent of indentation corners after the Vickers hardness test with a load of 500 g. The wear behavior was evaluated by CVMT-1000 multi-functional material friction and wear tester (sourced from Jinan Hengxu testing Machine Technology Co., LTD, Jinan, China). GCr15 steel balls were used as the grinding material, with a diameter of 5 mm, a rotation speed of 214 r/min, a loading load of 200 g, and a grinding time of 15 min. Before and after each wear test, the sample's weight was weighed using an electronic balance (MST-5000). The wear weight loss was obtained by using the weight before the wear test minus the weight after the test, and then the wear rate was calculated [24]. Meanwhile, the friction coefficient was recorded during the wear testing process. All wear tests were repeated three times for each case to ensure the reliability of the results. Finally, the overall view of the wear tracks was observed using an optical microscope (DMI-3000M) at a magnification of 50×.

3. Results and Discussion

3.1. Cross-Sectional Microstructure

Figure 1 presents the cross-sectional microstructure of nitrided samples treated by different plasma nitriding methods. It is clear a bright white layer was formed on the top surface after PN treatment, while a diffusion zone beneath this layer cannot be seen by optical microscopy. The bright white layer is also called a compound layer, and its thickness can be determined by measuring the layer thickness on the cross-sectional microstructure. It can be seen that under the same nitriding parameter of 520 °C/4 h, the compound layer thickness is in the range of 11.50–11.82 μm and 14.12–14.59 μm, and the average thickness is 11.64 μm and 14.32 μm for the conventional plasma nitriding treatment and aluminum-modified plasma nitriding, respectively. This illustrates that the thickness of the compound layer increases slightly due to aluminum modification under this condition. It needs to be noted that the compound layer thickness is in the range of 5.62–5.89 μm, and an average compound layer thickness of 5.75 μm is obtained by aluminum-modified plasma nitriding at 520 °C/0.5 h.

3.2. Surface Hardness and Effective Hardening Layer

Figure 2 depicts the variation in microhardness from the surface to the bulk material after different PN treatments and with the indentations inserted. The hardness is dependent on the diagonal size of the indentations. The inserted images show that, in all cases, the diagonal size of the indentation increases with the distance from the surface, which shows that the microhardness decreases with the distance from the surface. A much smaller

diagonal size of the indentations can be seen at the same distance from the surface for the 4 h Al-PN-treated sample, which corresponds to much higher hardness.

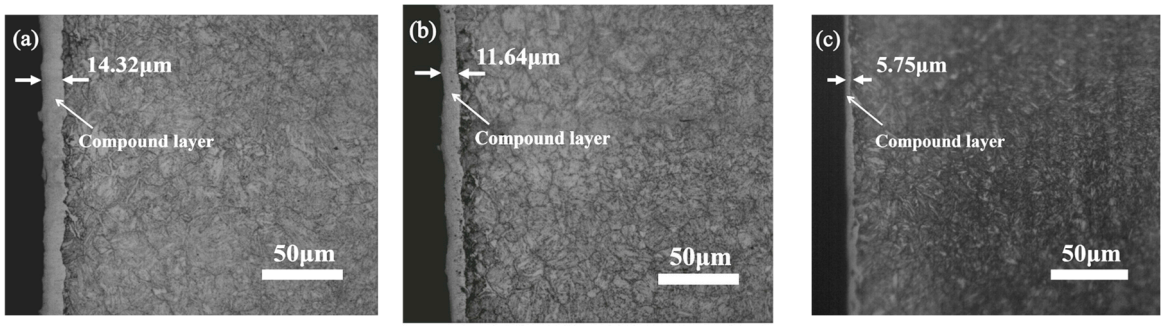

Figure 1. Cross-sectional microstructure of samples treated with different PN treatments: (**a**) 4 h Al-PN, (**b**) 4 h PN, (**c**) 0.5 h Al-PN.

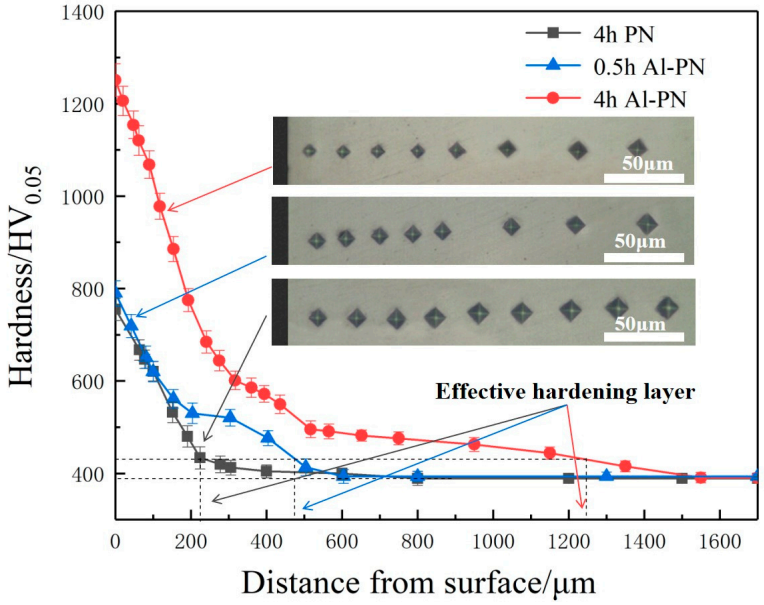

Figure 2. Cross-sectional microhardness of samples treated by different PN treatments.

The thickness of the effective hardening layer, also called case depth, is technically defined as the vertical distance from the very surface to the position at which the hardness is 50 HV higher than that of the substrate [27], and nitriding efficiency is determined by the thickness of effective hardening layer obtained per unit of time. It can be seen that the surface hardness and effective hardening layer are significantly enhanced following aluminum modification under the same process condition of 520 °C/4 h. The average surface hardness is increased from 755 $HV_{0.05}$ to 1251 $HV_{0.05}$, an enhancement of about 500 HV; the average effective hardening layer was dramatically increased from 224 μm to 1246 μm, an enhancement of more than 5 times, which illustrates that an ultra-high process efficiency was obtained with aluminum modification. It needs to be emphasized that a surface hardness of 790 $HV_{0.05}$ and an effective hardening layer of about 435 μm were formed by aluminum-modified plasma nitriding for only 0.5 h, which is higher than 755 $HV_{0.05}$ and almost twice as high as 224 μm achieved by traditional plasma nitriding after a much longer time of 4 h. Combined with the compound layer comparison shown in Figure 1, it can be concluded that a thinner compound layer and a thicker effective hardening layer can be obtained by Al-PN for 42CrMo steel, as well as higher surface hardness. It is known that the ideal characteristics of a nitriding layer for components

subjected to heavy wear and/or severe impact loads are a thicker effective hardening layer and a thinner compound layer.

3.3. XRD Analysis

The X-ray diffraction patterns of samples treated by conventional PN and Al-PN under the same process at 520 °C/4 h are shown in Figure 3. The data files used for XRD analysis are JCPDS-PDF: 83-0875 (γ'-Fe_4N), JCPDS-PDF: 76-0091 (ε-$Fe_{2-3}N$), JCPDS-PDF: 76-0566 (AlN), and JCPDS-PDF: 33-0020 (FeAl). It can be seen that patterns corresponding to AlN and FeAl appeared, which confirmed that phases of AlN and FeAl with high hardness were formed during Al-PN treatment because of aluminum modification, and the position and intensity of γ'-Fe_4N and ε-$Fe_{2-3}N$ were adjusted by Al-modification compared to those of conventional PN-treated samples. Combining this with the hardness comparison shown in Figure 2, a preliminary conclusion can be drawn that the ultra-high hardness of the Al-PN-treated layer is mainly attributed to the dispersion strengthening of hard phases formed in the nitriding layer.

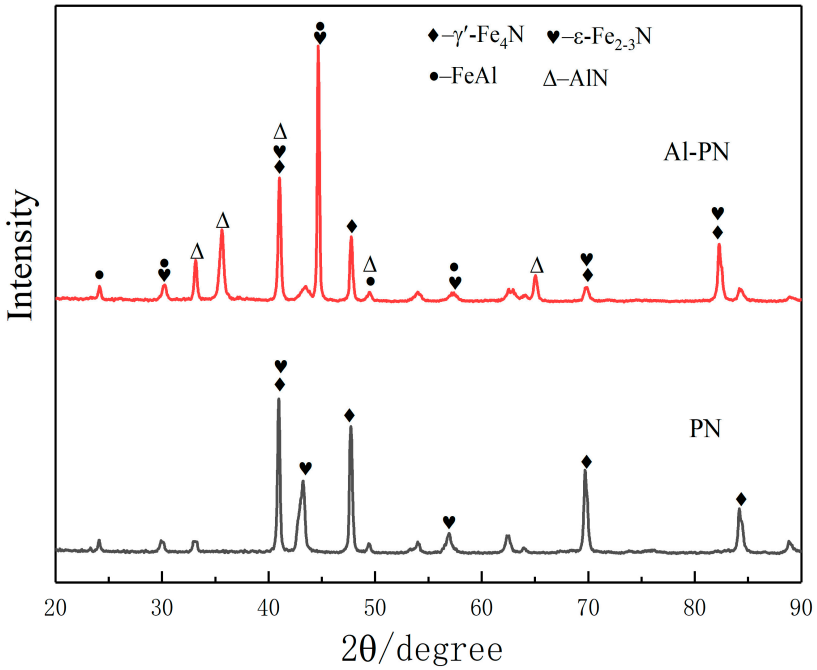

Figure 3. X-ray diffraction patterns of samples treated by PN and Al-PN at 520 °C/4 h.

3.4. Surface Morphology and Element Analysis

Figure 4 shows the surface morphology of samples treated by conventional PN and Al-PN under the same process at 520 °C/4 h, and the EDS element analysis is shown in Table 2. It can be seen that nitride particles are formed and distributed uniformly on the surface, and the EDS element analysis demonstrates that there exist 33.26% N and 9.38% Al on the surface of the Al-PN-treated sample, much higher than 23.28% N and no Al for the conventional PN-treated sample. This illustrates that aluminum modification during the PN process can not only cause Al atoms to be sputtered on the surface, but also cause many more N atoms to be absorbed on the surface due to the strong attraction of Al and N, thus promoting nitride particle formation and N diffusion inwards, leading to much higher hardness and a much thicker effective hardening layer. In other words, a much higher nitriding efficiency and better performance can be obtained by aluminum modification during the PN process.

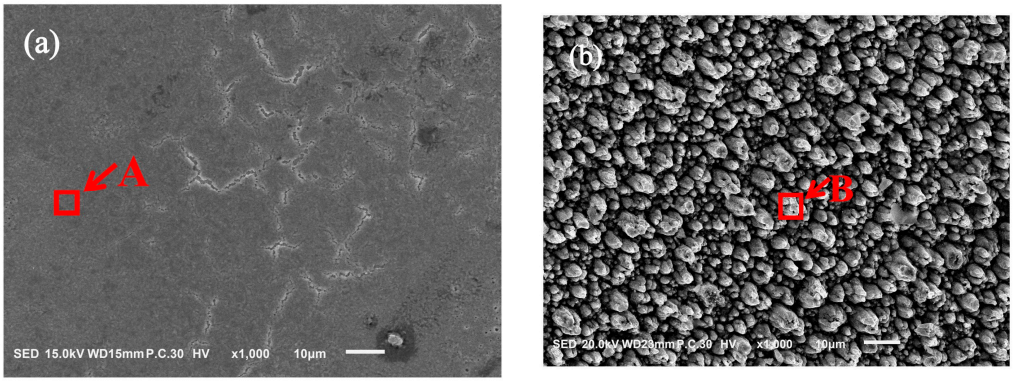

Figure 4. Surface morphology of samples nitrided at 520 °C/4 h. (**a**) Conventional PN; (**b**) Al-PN.

Table 2. EDS element analysis results, wt./%.

Sample	Area	Fe	Al	N
PN	A	76.72	/	23.28
Al-PN	B	57.36	9.38	33.26

3.5. Surface Topography and Roughness

It has been reported that surface topography and roughness have a significant influence on wear behavior, and the arithmetic mean value (Ra) is considered a representative parameter of surface roughness [25]. Figure 5 presents the 3D surface topography and roughness of samples treated by conventional PN and Al-PN under the same process at 520 °C/4 h. It can be determined that the surface roughness Ra of PN-treated and Al-PN-treated samples is 1.14 μm and 1.08 μm, respectively, i.e., the surface roughness is decreased by aluminum modification, which may be attributed to the formation of nitrides with a very small size at the top of the compound layer, as shown in Figure 4b.

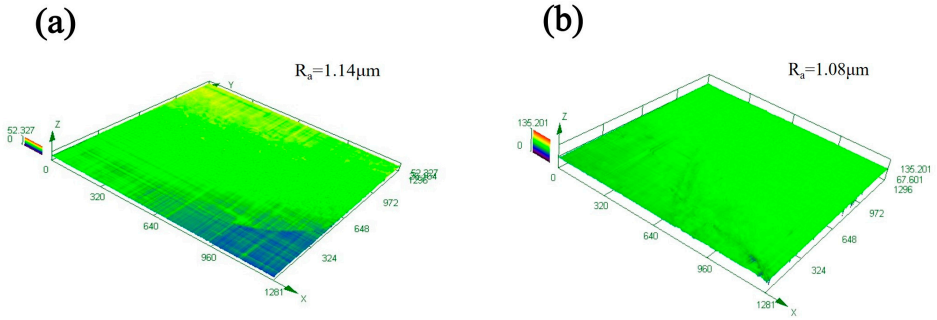

Figure 5. Three-dimensional surface topography and roughness of samples nitrided at 520 °C/4 h. (**a**) Conventional PN; (**b**) Al-PN.

3.6. Wear Behavior

Figure 6 shows the friction coefficient of samples treated by conventional PN and Al-PN under the same process at 520 °C/4 h. It can be seen that the friction coefficient of PN-treated and Al-PN-treated samples is 0.75 and 0.64, respectively, i.e., the friction coefficient is decreased and the friction coefficient curve is more stable for the Al-PN-treated sample, which may be attributed to the corresponding lower surface roughness, as shown in Figure 5. This is because it is reported that surface roughness has more of an effect on the friction coefficient than hardness; a lower surface roughness tends to bring about a lower friction coefficient [25].

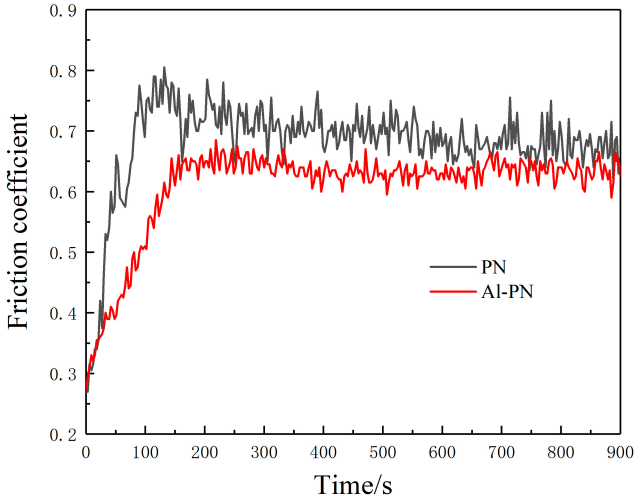

Figure 6. Friction coefficient comparison of samples treated by PN and Al-PN at 520 °C/4 h.

Whole pictures of wear marks are visible proof showing the extent of wear. Figure 7 shows whole pictures of wear marks of nitrided samples treated by conventional PN and Al-PN at 520 °C/4 h. It demonstrates that the wear marks are much wider for the conventional PN-treated sample, and with a lot of grinding, grooving, and pits on the worn surface, while the wear marks are much narrower for the Al-PN-treated sample, with noticeably fewer worn pits. By comparing the wear marks in both cases, it is clear that wear resistance is enhanced by Al-PN.

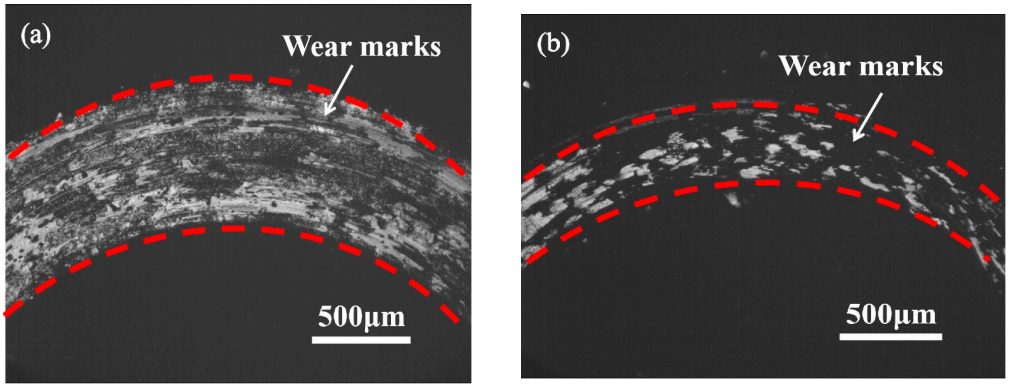

Figure 7. The whole picture of wear marks of samples treated by PN and Al-PN at 520 °C/4 h. (**a**) PN; (**b**) Al-PN.

In order to make a quantitative comparison of the wear behavior between PN- and Al-PN-treated samples, the wear rate $\delta = \frac{m_1 - m_2}{N \cdot L}$ in both cases was determined according to the following formula [17]:

$$\delta = \frac{m_1 - m_2}{N \cdot L} \quad (1)$$

where m_1, m_2, N, and L are the sample's weight before and after the wear test, the applied load, and the sliding distance, respectively.

As shown in Figure 8, the wear rate of samples treated by PN and Al-PN is 8.15×10^{-5} g·N^{-1}·m^{-1} and 4.07×10^{-5} g·N^{-1}·m^{-1}, respectively, i.e., the wear rate of the Al-PN-treated sample is decreased by half, which means that the wear resistance is enhanced by about 2 times due to aluminum modification. The extent of the decrease in the wear rate agrees well with the surface hardness data shown in Figure 8.

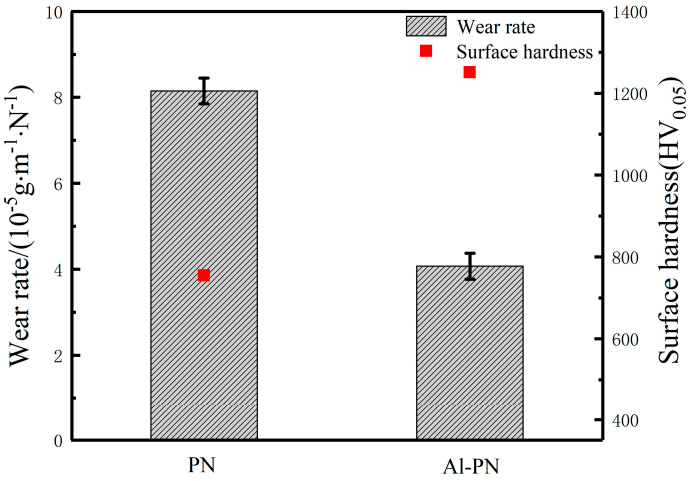

Figure 8. Comparison of wear rate between samples treated by PN and Al-PN at 520 °C/4 h, with surface hardness shown.

3.7. Brittleness Analysis

Brittleness refers to the tendency of a metal to break without being significantly distorted once exposed to a high level of stress. Based on the Chinese national standard [27], the brittleness level of a nitriding layer is divided into five grades according to the cracking extent of the indentation after a Vickers hardness test. These grades are as follows: Grade 5 brittleness represents the most brittle metals, with severe cracking on four sides and/or corners of the indentation; Grade 4 brittleness corresponds to cracking on three sides and/or corners; Grade 3 brittleness corresponds to cracking on two sides and/or corners; Grade 2 brittleness corresponds to cracking on one side and/or corner; and Grade 1 brittleness means the least brittle metal, corresponding to no cracking around all the indentation, and thus representing the best toughness. Generally, Grade 1 brittleness is needed for components subjected to heavy impact loads in order for them to have a long service life.

The indentations of samples treated by conventional PN and Al-PN under the same process at 520 °C/4 h are shown in Figure 9. It can be seen that there exists severe cracking on three sides and corners around the indentation of the PN-treated sample, so the brittleness is determined to be Grade 4 [27], while there is no cracking around the indentation of the Al-PN-treated sample, so its brittleness is determined to be Grade 1 [27]. Therefore, a conclusion can be drawn that the brittleness grade can be effectively decreased by the addition of aluminum; in other words, toughness can be effectively improved, and the strict technical requirements of both excellent wear resistance and toughness for the components can be met.

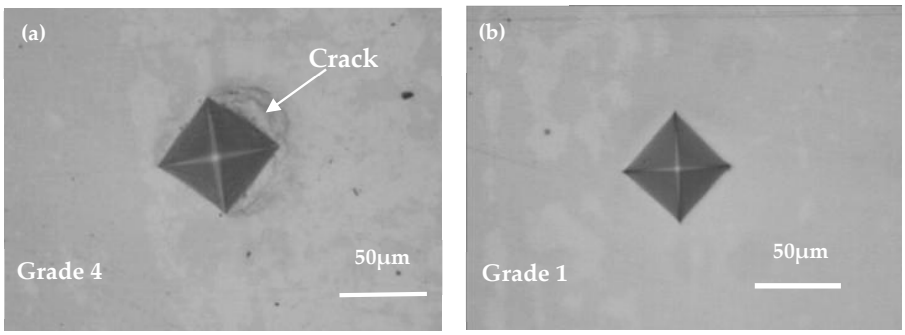

Figure 9. Comparison of indentations between samples treated by PN and Al-PN at 520 °C/4 h. (**a**) PN; (**b**) Al-PN.

Meanwhile, it can be seen that the indentation area of the Al-PN-treated sample is much smaller than that of the PN-treated sample, which also implies that the surface

hardness is significantly enhanced by aluminum modification, which is consistent with the results shown in Figures 2 and 8.

4. Mechanism and Discussions

In order to have a comprehensive and systematic understanding of the amazing effect of aluminum modification on plasma nitriding, the main research results are summarized and compared in Table 3. It shows that the effective hardening layer (corresponding to nitriding efficiency) can be dramatically enhanced by aluminum modification. More valuably, both the wear resistance and toughness are greatly enhanced by Al-PN due to the much higher hardness and much lower ratio of compound layer thickness to effective hardening layer thickness.

Table 3. Comparison of nitriding layer characteristics and comprehensive performance of Al-PN and PN-treated samples at 520 °C/4 h.

Process	Average Compound Layer Thickness (μm)	Effective Hardening Layer Thickness (μm)	Ratio of Compound Layer to Effective Hardening Layer	Average Surface Hardness ($HV_{0.05}$)	Wear Rate (10^{-5} g·N^{-1}·m^{-1})	Brittleness Level	Phase Constituents
PN	11.64	224	0.052	755	8.15	4	$Fe_{2-3}N$, Fe_4N
Al-PN	14.32	1246	0.011	1251	4.07	1	$Fe_{2-3}N$, Fe_4N, AlN, FeAl

Note: nitriding efficiency is determined according to the effective hardening layer formed per unit of time.

The possible mechanism for the amazing effect of aluminum modification on the nitriding efficiency and performance described above is explained in the following paragraphs.

During the plasma nitriding process, ionization happens in the thin gas atmosphere resulting from the influence of a high-voltage DC electric field, forming a plasma region composed of N^+, H^+, e^- and N, H active atoms, where N^+ and H^+ ions are bombarded towards the cathode at a very high speed under a strong electric field in the plasma region. High-velocity bombardment makes Fe and Al ions splash out to the plasma region.

Due to the strong attraction between Al and N, many more N atoms are absorbed on the surface, as confirmed by EDS in Table 2. On the one hand, a high content of N has a strong tendency to react with Al to form microparticles of AlN with very high hardness; on the other hand, a much higher N gradient can dramatically increase the diffusion rate of nitrogen atoms, thus bringing about much longer diffusion distances and stronger solution-strengthening effects. Meanwhile, a part of the active Al atoms can also react with Fe to form FeAl; thus, the strong dispersion-strengthening effect of AlN and FeAl brings about a significant enhancement of hardness in the nitriding layer. Therefore, both the surface hardness and the effective hardening layer can be dramatically enhanced due to the dispersion strengthening and stronger solution hardening that result from the effect of aluminum modification, which brings about excellent wear behavior.

Meanwhile, the brittleness level is greatly decreased due to the obvious decrease in the ratio of compound layer thickness to effective hardening layer thickness. In other words, the toughness of the nitriding layer is greatly enhanced, which is of significant value for components subjected to severe impact loads.

5. Conclusions

Aluminum-modified plasma nitriding was primarily developed by the addition of a few FeAl particles around the samples during the plasma nitriding process, and the amazing effect of aluminum modification on both nitriding efficiency and related properties was investigated for 42CrMo alloy steel. The following main conclusions can be drawn compared with conventional plasma nitriding:

1. Nitriding efficiency was improved by aluminum modification by about 6 times, with the effective hardening layer increasing from 224 μm to 1246 μm when treated at 520 °C/4 h. Higher surface hardness and a thicker effective hardening layer were obtained for samples Al-PN treated for 0.5 h compared to those PN treated for 4 h.
2. The surface hardness was increased from 755 $HV_{0.05}$ to 1251 $HV_{0.05}$ and the wear rate was reduced from 8.15×10^{-5} g·N^{-1}·m^{-1} to 4.07×10^{-5} g N^{-1} m^{-1}, i.e., the wear resistance wan enhanced by almost 2 times after being treated at 520 °C/4 h.
3. The brittleness grade was greatly decreased by Al-PN due to the much lower ratio of compound layer thickness to effective hardening layer thickness; in other words, the toughness was effectively improved.
4. The innovative technology developed in this study can not only greatly enhance nitriding efficiency, and thus save time and cost, but also improve the service life of the treated components due to their much better performance.

Author Contributions: Z.H.: Conceptualization and Methodology. W.W.: Investigation, Help with the Experiments. J.H.: Supervision, Writing—Review and Editing. J.G.: Visualization, Investigation, Software, Validation, and Second Supervisory Role. All authors have read and agreed to the published version of the manuscript.

Funding: This work was supported by the National Natural Science Foundation of China (21978025), PAPD & TAPP, and the Postgraduate Research & Practice Innovation Program of Jiangsu Province (SJCX24_1580).

Institutional Review Board Statement: Not applicable.

Informed Consent Statement: Not applicable.

Data Availability Statement: Data are contained within the article.

Conflicts of Interest: The authors declare no conflict of interest.

References

1. Liu, R.L.; Yan, F.Y.; Yan, M.F. Surface grain nanocrystallization of Fe-Cr-Ni alloy steel by plasma thermochemical treatment. *Surf. Coat. Tech.* **2019**, *370*, 136. [CrossRef]
2. Li, J.; Hong, H.H.; Sun, L.; Yang, Y.; Li, D.Y.; Zhang, S.H. Argon ion sputtering bridging plasma nitriding and GLC film deposition: Effects on the mechanical and tribological properties. *Surf. Coat. Tech.* **2024**, *479*, 130559. [CrossRef]
3. Ni, J.; Ma, H.; Wei, W.; An, X.L.; Yu, M.H.; Hu, J. Novel Effect of Post-Oxidation on the Comprehensive Performance of Plasma Nitriding Layer. *Coatings* **2024**, *14*, 86. [CrossRef]
4. Hong, H.H.; Xie, G.R.; Sun, L.; Yang, Y.; Zhang, Z.; Li, J.; Zhang, S.H. The diffusion behavior and surface properties of catalytic nitriding with LaFeO3 film prepared by the sol-gel method. *Surf. Coat. Tech.* **2023**, *467*, 129720. [CrossRef]
5. Lu, J.S.; Li, B.K. Discussion of precision heat treatment and anti-fatigue manufacturing of gear. *J. Mech. Eng.* **2019**, *43*, 170–175.
6. Li, J.; Tao, X.; Wu, W.; Xie, G.; Yang, Y.; Zhou, X.; Zhang, S. Effect of arc current on the microstructure, tribological and corrosion performances of AISI 420 martensitic stainless steel treated by arc discharge plasma nitriding. *J. Mater. Sci.* **2023**, *58*, 2294. [CrossRef]
7. Wang, B.; Liu, B.; Zhang, X.D.; Gu, J.F. Enhancing heavy load wear resistance of AISI 4140 steel through the formation of a severely deformed compound-free nitrided surface layer. *Surf. Coat. Tech.* **2018**, *356*, 89. [CrossRef]
8. Shen, J.H.; Hu, J.; An, X.L. Regulation of phase partition and wear resistance for FeCoCrV high entropy alloy by heat treatment. *Intermetallics* **2024**, *167*, 108232. [CrossRef]
9. Wang, Z.Y.; Xing, Z.G.; Wang, H.D.; Li, G.L.; Liu, K.J.; Xing, Z. Research status of test method for bending fatigue life of heavy duty gear. *Mater. Rev.* **2018**, *32*, 3051.
10. He, Z.; Jia, W.J.; Liu, X.L.; Wang, D.D.; Hu, J. The effect of aluminum addition on plasma nitriding for 42CrMo steel. *Mater. Lett.* **2024**, *377*, 137440. [CrossRef]
11. Li, L.Z.; Liu, R.L.; Liu, Q.L.; Wu, Z.J.; Meng, X.L.; Fang, Y.L. Effects of Initial Microstructure on the Low-Temperature Plasma Nitriding of Ferritic Stainless Steel. *Coatings* **2022**, *12*, 1404. [CrossRef]
12. Chen, W.L.; Huang, Y.H.; Xiao, H.; Meng, X.N.; Li, Z.; Chen, Z.X.; Hong, Y.; Wu, C.L. The thermal process for hardening the nitrocarburized layers of alow-carbon steel. *Scr. Mater.* **2022**, *210*, 114467. [CrossRef]
13. Zdravecka', E.; Slota, J.; Solfronk, P.; Kolnerová, M. Evaluation of the Effect of Different Plasma-Nitriding Parameters on the Properties of Low-Alloy Steel. *J. Mater. Eng. Perform.* **2017**, *26*, 3588. [CrossRef]
14. Yan, M.F.; Chen, B.F.; Li, B. Microstructure and mechanical properties from an attractive combination of plasma nitriding and secondary hardening of M50 steel. *Appl. Surf. Sci.* **2018**, *455*, 1. [CrossRef]

15. Kim, Y.M.; Son, S.W.; Lee, W.B. Thermodynamic and kinetic analysis of formation of compound layer during gas nitriding of AISI1018 carbon steel. *Met. Mater. Int.* **2018**, *24*, 180. [CrossRef]
16. Saeed, A.; Khan, A.W.; Jan, F.; Shah, H.U.; Abrar, M.; Zaka-UI-Islam, M.; Khalid, M.; Zakaullah, M. Optimization study of pulsed DC nitrogen-hydrogen plasma in the presence of an active screen cage. *Plasma Sci. Technol.* **2014**, *16*, 460. [CrossRef]
17. Zhang, C.W.; Wen, K.; Gao, Y. Low-temperature plasma nitriding at 500 °C on surface-nanocrystalline Ti–4Al–2V alloy. *Mater. Chem. Phys.* **2023**, *306*, 128080. [CrossRef]
18. Nishimoto, A.; Nagatsuka, K.; Narita, R.; Nii, H.; Akamatsu, K. Effect of the distance between screen and sample on active screen plasma nitriding properties. *Surf. Coat. Tech.* **2010**, *205*, S365. [CrossRef]
19. Naeem, M.; Torres, A.V.R.; Serra, P.L.C.; Monção, R.M.; Junior, C.A.A.; Rossino, L.S.; Costa, T.H.C.; Costa, C.L.S.C.; Iqbal, J.; Sousa, R.R.M. Combined plasma treatment of AISI-1045 steel by hastelloy deposition and plasma nitriding. *J. Build. Eng.* **2022**, *47*, 103882. [CrossRef]
20. Zhang, Z.X.; Li, X.Y.; Dong, H.S. Plasma-nitriding and characterization of FeAl40 iron aluminide. *Acta Mater.* **2015**, *86*, 341. [CrossRef]
21. Gonzalez-Moran, A.K.; Naeem, M.; Hdz-García, H.M.; Granda-Gutiérrez, E.E.; Ruíz-Mondragón, J.J.; Alvarez-Vera, M.; Díaz-Guillén, J.C. Improved mechanical and wear properties of H13 tool steel by nitrogen-expanded martensite using current-controlled plasma nitriding. *J. Mater. Res. Technol.* **2023**, *25*, 4139. [CrossRef]
22. Shen, H.Y.; Wang, L. Oxide layer formed on AISI 5140 steel by plasma nitriding and post-oxidation in a mixture of air and ammonia. *J. Alloy Compd.* **2019**, *806*, 1517. [CrossRef]
23. Koutná, N.; Löfler, L.; Holec, D.; Chen, Z.; Zhang, Z.; Hultman, L.; Mayrhofer, P.H.; Sangiovanni, D.G. Atomistic mechanisms underlying plasticity and crack growth in ceramics: A case study of AlN/TiN superlattices. *Acta Mater.* **2022**, *229*, 117809. [CrossRef]
24. Sun, J.Q.; Wang, D.R.; Yang, J.; Li, F.; Zuo, L.; Ge, F.; Chen, Y. In Situ Preparation of Nano-Cu/ Microalloyed Gradient Coating with Improved Antifriction Properties. *Coatings* **2022**, *12*, 1336. [CrossRef]
25. Chen, H.; Wang, W.L.; Le, K.; Liu, Y.Z.; Gao, X.M.; Luo, Y.; Zhao, X.; Liu, X.N.; Xu, S.S.; Liu, W.M. Effects of substrate roughness on the tribological properties of duplex plasma nitrided and MoS2 coated Ti6Al4V alloy. *Tribol. Int.* **2024**, *191*, 109123. [CrossRef]
26. Kang, Q.F.; Wei, K.X.; Fan, H.M.; Liu, X.L.; Hu, J. Ultra-high efficient novel plasma aluminum-nitriding methodology and performances analysis. *Scr. Mater.* **2022**, *220*, 114902. [CrossRef]
27. *GB/T 11354-2005*; Determination of Nitrided Case Depth and Metallographic Microstructure Examination for Steel and Iron Parts. Standardization Administration of China, National standard of the People's Republic of China: Beijing, China, 2005.